

Dynamical phase transition in the first-passage probability of a Brownian motion

B. Besga, F. Faisant, A. Petrosyan, S. Ciliberto*
Univ Lyon, ENS de Lyon, Univ Claude Bernard, CNRS,
Laboratoire de Physique, UMR 5672, F-69342 Lyon, France

Satya N. Majumdar†
LPTMS, CNRS, Univ. Paris-Sud, Université Paris-Saclay, UMR 8626, 91405 Orsay, France
(Dated: April 22, 2021)

We study the first-passage time distribution (FPTD) $F(t_f|x_0, L)$ for a freely diffusing particle starting at x_0 in one dimension, to a target located at L , averaged over the initial position x_0 drawn from a normalized distribution $(1/\sigma)g(x_0/\sigma)$ of finite width σ . We show the averaged FPTD undergoes a sharp dynamical phase transition from a two-peak structure for $b = L/\sigma > b_c$ to a single peak structure for $b < b_c$. This transition is generated by the competition of two characteristic time scales σ^2/D and L^2/D , where D is the diffusion coefficient. A very good agreement is found between theoretical predictions and experimental results obtained with a Brownian bead whose diffusion is initialized by an optical trap which determines the initial distribution $g(x_0/\sigma)$. We show that this transition is robust: it is present for all initial conditions with a finite σ , in all dimensions, and also exists for more general stochastic processes going beyond free diffusion.

First-passage properties of stochastic processes are fundamental to understand many important phenomena in nature and have wide ranging applications across fields [1, 2]. These include estimating reaction rates in chemical processes [3, 4], understanding persistence properties in nonequilibrium systems [5, 6], computing efficiencies of search algorithms [7, 8], estimating the statistics of extreme events [9] and records in a time series [10–12], numerous applications in biology [13–15], astrophysics [16] and computer science [17].

In particular, the first-passage properties of a simple random walk or a Brownian motion have been widely studied, not only as a simple solvable example, but due to its plethora of applications. One recent application that has created much interest is in the context of a random walk or a Brownian motion subjected to resetting to its initial starting point, either at random times [18–23] or periodically [24, 25]. Repeated resetting to its starting position of a freely diffusing Brownian particle has two major effects: (i) it drives the particle to a nonequilibrium steady state so that its position distribution becomes stationary at long times (ii) the mean first-passage times to a fixed target becomes finite. Moreover, an optimal resetting rate was found that makes the mean first-passage time minimal, thus rendering a diffusive search an efficient search process via resetting [18]. This led to an enormous recent activities in the field, both theoretically [8] and more recently, experimentally [26, 27].

There are however two ways in which realistic situations differ from the assumptions used in these theoretical models: (a) it is impossible to reset the particle to its starting point ‘instantaneously’ as was assumed in the original models (b) it is physically impossible to reset the particle exactly to its starting point. The latter situation arises in particular in experiments conducted with optical tweezers [26, 27], where a particle is usually trapped in an external confining potential (optical trap), typically harmonic. At thermal equilibrium, the stationary position distribution of the particle is thus a Gaussian with a finite width σ (which depends on the temperature

T and the stiffness of the laser trap κ as $\sigma^2 = k_B T / \kappa$). The particle is initially prepared in thermal equilibrium in the trap and then the trap is switched off and the particle undergoes free diffusion during a certain period. After this period, the trap is again switched on and the particle is allowed to relax to its thermal equilibrium before the trap is switched off again. The relaxation to thermal equilibrium where the particle is driven towards the trap center mimics the ‘resetting’ (which is thus non-instantaneous). However, under this mechanism, the particle never goes back exactly to its starting position, but its new starting position for the subsequent diffusive phase is effectively chosen from a Gaussian distribution with a finite width σ . The case $\sigma = 0$ (delta function) would correspond exactly to resetting to the fixed initial position. But in realistic situations, σ is always finite.

Several recent theoretical studies have addressed the issue (a) that a physical resetting is always non-instantaneous and the effect of a finite duration of the resetting period is well understood [28–33]. On the experimental side the development of protocols accelerating the dynamics of optically trapped colloids [34, 35] could lead to a drastic reduction of the resetting period. However, equally important is issue (b), i.e, how a finite width σ in the initial position distribution may affect the first-passage properties of the Brownian motion under resetting? Indeed, in the experiment reported in Ref. [27], the presence of a finite σ was found to alter *substantially* the mean first-passage time to the target.

The purpose of this Letter is to demonstrate that a finite width σ in the initial position distribution of a Brownian particle profoundly affects its first-passage time distribution (FPTD), even in the absence of resetting! We start with an extremely simple system: just a free Brownian motion in 1d with a diffusion constant D , starting from x_0 , with a target located at L (see Fig. 1a). The FPTD $F(t|x_0, L)$ to the target for fixed x_0 is well known [1, 6]. Now we just average over the initial position x_0 drawn from, say a Gaussian distribution $\mathcal{P}(x_0) = e^{-x_0^2/2\sigma^2} / \sqrt{2\pi\sigma^2}$ with a finite σ , corresponding to

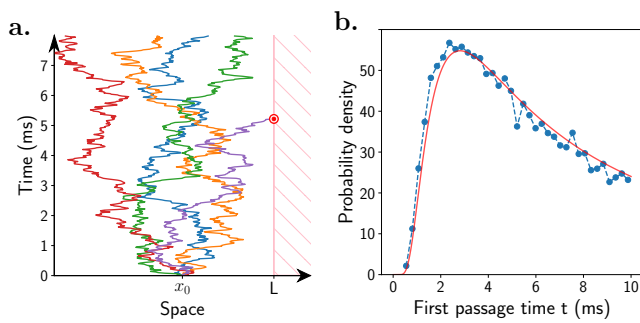


FIG. 1: **a.** Experimental trajectories of a Brownian motion on a line starting at x_0 with a fixed target at L (parameters : $L - x_0 = 50$ nm and $D = 1.5 \times 10^{-13}$ m².s⁻¹). **b.** First-passage probability density $F(t|0,L) = (L/\sqrt{4\pi Dt^3})e^{-L^2/4Dt}$, plotted as a function of t (red continuous line) for $L = 50$ nm and $D = 1.5 \times 10^{-13}$ m².s⁻¹ corresponding to the experimental data (blue dots) obtained for 1.8×10^4 first-passages.

the equilibrium distribution in a harmonic trap before the trap is switched off. We show that just this simple averaging leads to a profound change in the FPTD. We have implemented an experiment where we can follow the trajectories of a free Brownian particle from an initial gaussian distribution as a result of the optical trapping. The experimental setup is detailed in [27] and consists in an infrared laser beam tightly focused into a microfluidic chamber to trap a silica micro-sphere of radius $R = 1$ μ m in water. The position of the Brownian particle is read from the deviation of a red laser on a quadrant photodiode at 50 kHz. The stiffness of the trap is chosen by changing the trapping laser intensity power thanks to an electro-optical modulator. In particular after equilibration the trap is switched off to follow the free diffusion (see Fig. 1a) and the protocol is repeated to acquire statistics on the first passage times.

Our main results are summarised as follows. A finite σ introduces a new time scale $t_1^* \sim O(\sigma^2/D)$ and for $t \leq t_1^*$ the averaged FPTD develops an anomalous regime. First, the averaged FPTD diverges as $t^{-1/2}$ as $t \rightarrow 0$. Secondly, as time increases, the FPTD decreases, achieves a minimum at $t \sim t_1^*$, then increases and achieves a maximum at $t_2^* \sim O(L^2/D)$, before finally decaying as $t^{-3/2}$ when $t \gg O(L^2/D)$. Thirdly, and most remarkably, there exists a critical value $\sigma = \sigma_c$ such that for $\sigma > \sigma_c$, the minimum at t_1^* and the maximum at t_2^* both disappear and distribution decays monotonically to 0 as $t \rightarrow \infty$. We derive this result analytically, and demonstrate that both the simulation and the experimental data match perfectly our theoretical predictions. We also provide a physical meaning of this anomalous regime and the associated transition at $\sigma = \sigma_c$: we show that for $\sigma < \sigma_c$ when $t_1^* \ll t_2^*$, the anomalous early time regime in FPTD is caused by rare trajectories that start very close to the target at L . For $t_1^* \ll t_2^*$, such rare atypical trajectories are well separated in time scales from typical trajectories that start close to the origin. The transition at $\sigma = \sigma_c$ occurs when these two time scales t_1^* and t_2^* merge with other. In this sense, this phase transition is ‘dynamical’. We

then show that this phase transition is robust and happens for any unbounded initial distribution with a finite width σ , not necessarily a Gaussian. Furthermore, we argue and verify numerically that this transition is not limited to one dimension, and occurs even in higher dimensions. Our results are particularly striking since the underlying system and its associated physics is really very simple.

We start with a Brownian particle on a line with diffusion constant D , in the presence of a fixed target at L . The particle starts at the initial position x_0 (which can be on either side of L). Let $F(t|x_0,L)dt$ denote the probability that the particle finds the target for the first time in $[t, t + dt]$, given fixed x_0 and L . This FPTD $F(t|x_0,L)$ can be computed very simply [1, 6]. Let $P(x,x_0,t)$ denote the probability density that the particle reaches x at time t , starting from x_0 and does not cross L in time t . Let us consider $x_0 \leq L$ (the case $x_0 \geq L$ can be similarly computed). Then $P(x,x_0,t)$ satisfies the standard Fokker-Planck equation, $\partial_t P = D \partial_x^2 P$, for $x \leq L$ with absorbing boundary condition at the target $P(x=L, x_0, t) = 0$. The solution can be obtained using the method of images [1]

$$P(x, x_0, t) = \frac{1}{\sqrt{4\pi Dt}} \left[e^{-(x-x_0)^2/4Dt} - e^{-(x+x_0-2L)^2/4Dt} \right]. \quad (1)$$

Interpreting each trajectory, starting from x_0 , as an independent Brownian particle, the FPTD is given simply by the flux of such independent surviving particles through $x = L$ at time t , $F(t|x_0, L) = -D \partial_x P(x, x_0, t) \Big|_{x=L}$. Using (1), one gets

$$F(t|x_0, L) = -\partial_t S(t|x_0, L) = \frac{|L-x_0|}{\sqrt{4\pi Dt^3}} e^{-(L-x_0)^2/4Dt}. \quad (2)$$

Suppose that x_0 is fixed, say at $x_0 = 0$. Then Eq. (2) gives, $F(t|0, L) = \frac{L}{\sqrt{4\pi Dt^3}} e^{-L^2/4Dt}$. As a function of t (see Fig. 1b) for a plot), $F(t|0, L)$ has very different behavior across the time scale $t_2^* = L^2/2D$. It decays algebraically as $t^{-3/2}$ for $t \gg t_2^* = L^2/2D$. This is caused by trajectories that start at 0, but typically diffuse away in the opposite direction and finally reaches L at times $t \gg t_2^*$. In contrast, for $t \ll t_2^*$, it vanishes extremely rapidly in an essential singular way $\sim e^{-L^2/4Dt}$ as $t \rightarrow 0$. This behavior is also easy to understand physically. The trajectories that reach L at early times, starting from 0, are those that move *ballistically* from 0 to L in time t . Indeed, the statistical weight of a Brownian trajectory is $\propto \exp[-1/(4Dt) \int_0^t (dx/d\tau)^2 d\tau]$. For ballistic trajectories, $dx/d\tau = L/t$ and hence the flux of such trajectories contribute $\propto e^{-L^2/4Dt}$ which exactly reproduces the small t behavior of $F(t|0, L)$. Experimentally we compile the first passage times of the Brownian particle at a target situated at $L - x_0 = 50$ nm away from its initial position and find a very good agreement with the theoretical FPTD $F(t|0, L)$ (see Fig. 1b).

What happens when the initial position x_0 is not fixed, but drawn from a distribution $\mathcal{P}(x_0)$? Averaging the FPTD $F(t|x_0, L)$ in (2) over x_0 , we get

$$\bar{F}(t|\sigma, L) = \int_{-\infty}^{\infty} F(t|x_0, L) \mathcal{P}(x_0) dx_0. \quad (3)$$

For the Gaussian distribution $\mathcal{P}(x_0) = e^{-x_0^2/2\sigma^2}/\sqrt{2\pi\sigma^2}$, the integration in (3) can be performed explicitly. In terms of the dimensionless variables, $\tau = \frac{2Dt}{\sigma^2}$ and $b = \frac{L}{\sigma}$, the averaged FPTD in (3) can be expressed in the scaling form

$$\bar{F}(t|\sigma, L) = \frac{2D}{\sigma^2} \Phi\left(\frac{2Dt}{\sigma^2} = \tau, \frac{L}{\sigma} = b\right), \quad (4)$$

where the scaling function

$$\Phi(\tau, b) = \frac{1}{\pi\sqrt{\tau}(1+\tau)} \left[e^{-b^2/2} + \sqrt{\frac{\pi b^2 \tau}{2(1+\tau)}} e^{-b^2/2(1+\tau)} \times \operatorname{erf}\left(\sqrt{\frac{b^2 \tau}{2(1+\tau)}}\right) \right] \quad (5)$$

The average FPTD is plotted in Fig. (2) vs. time for different values of b . In (5), for any fixed b , the function $\Phi(\tau, b)$ diverges as $\tau^{-1/2}$ as $\tau \rightarrow 0$ (the first term dominates). Remarkably there is a critical value $b_c = 2.279\dots$ such that for $b > b_c$, there are two time scales $\tau_1^* \sim O(1)$ and $\tau_2^* \sim O(b^2)$ (in original time t they correspond to $t_1^* \sim O(\sigma^2/D)$ and $t_2^* \sim O(L^2/D)$ respectively). The FPTD scaling function decreases with increasing τ and achieves a minimum at τ_1^* , then increases and achieves a maximum at τ_2^* before finally decaying as $\tau^{-3/2}$ for $\tau \gg \tau_2^*$, thus creating a horizontal S-shaped curve visible in Fig. (2) for $\bar{F}(t|\sigma, L)$. As $b \rightarrow b_c$, the two time scales merge and for $b > b_c$, the scaling function decays monotonically with increasing τ . Thus just a simple averaging over the initial condition leads to a rather rich FPTD, including a ‘dynamical’ phase transition at $b = b_c$ caused by the merging of two time scales. The critical value b_c can be precisely determined as follows. If we plot the derivative $\partial_\tau \Phi(\tau, b)$ as a function τ or $b > b_c$, it vanishes at the two roots τ_1^* and τ_2^* , corresponding respectively to the minimum and maximum in Fig. (2). As $b \rightarrow b_c$, the two roots approach each other and at $b = b_c$, they merge. Consequently at $b = b_c$, both the first and the second derivatives of $\Phi(\tau, b)$ (with respect to τ) vanish at $\tau_1^* = \tau_2^* = \tau^*$. Solving these two equations (using Mathematica software) for the two unknowns τ^* and b_c , we get $b_c \approx 2.279$.

Experimentally the Brownian particle is optically trapped in a harmonic potential leading to a equilibrium Gaussian distribution in the trap with $\sigma = 36$ nm. We release the particle from the trap 5×10^4 times and measure the average FPTD for different target positions. Our experimental results match very well the theoretical predictions (see Fig. (2)) and the dynamical phase transition associated.

The physics behind this rather striking behavior of the FPTD can be understood as follows. We can think of the trajectories of the single Brownian particle as an assembly of independent Brownian particles with different starting points x_0 and different histories. Let us first assume that $L \gg \sigma$, i.e., $b \gg 1$ so that the two time scales $\tau_1^* \sim O(1)$ and $\tau_2^* \sim O(b^2)$ are well separated with $\tau_1^* \ll \tau_2^*$. We consider the different parts of the horizontal S-shaped FPTD in Fig. (2).

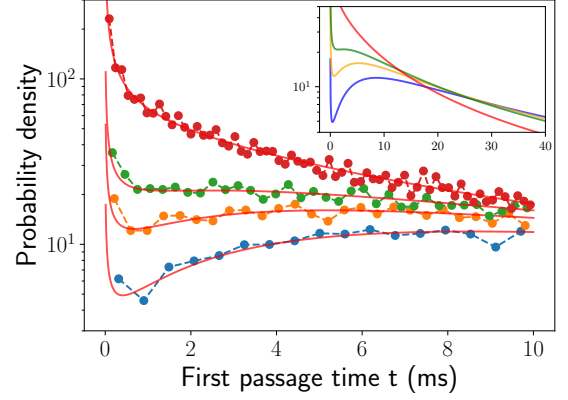


FIG. 2: Theoretical (red lines) an experimental (dots) FPTD $\bar{F}(t|\sigma, L)$ in (4), for Gaussian initial condition ($\sigma = 36$ nm), plotted as a function of t for $b = 3, 2.6, 2.3$ and 1.4 (from bottom to top) obtained from $4.7 \times 10^3, 7.9 \times 10^3, 9.1 \times 10^3$ and 1.7×10^4 first passages time measurements respectively. For any finite b the scaling function diverges as $t^{-1/2}$ as $t \rightarrow 0$. For $b > b_c = 2.279$, the function decreases as t increases and achieves a minimum at $t_1^* \sim O(\sigma^2)$. It then increases and achieves a maximum at $t_2^* \sim O(L^2)$ and then decays algebraically as $t^{-3/2}$ for $t \gg t_2^*$ (see inset). As $b \rightarrow b_c$ the two time scales merge and for $b < b_c$, the function decreases monotonically with increasing t . Inset : longer timescale for theoretical FPTD as function of t in ms (same parameters than the main figure).

- Anomalous regime $0 \leq \tau \leq \tau_1^*$: when time τ is small, the particles that arrive at L for the first time in $[\tau, \tau + d\tau]$ are the ones that diffuse from the starting points in the vicinity of the target L . Essentially, the particles that initially are in the region $[L - \sqrt{2Dt}, L + \sqrt{2Dt}]$ will contribute to this flux at L at time t . Thus integrating Eq. (3) over this region, it is easy to see that one gets $\Phi(\tau, b) \sim e^{-b^2/2}/\sqrt{\tau}$. The weight factor $e^{-b^2/2} = e^{-L^2/2\sigma^2}$ is just the probability of having a particle at $x_0 = L$ in the initial condition. Hence in this regime, the first term in (5) dominates. A similar $\tau^{-1/2}$ divergence at short times also occurs in diffusion controlled reactions with uniform initial concentration [1].
- When $\tau_1^* \leq \tau \leq \tau_2^*$: As time exceeds $\tau_1^* \sim O(1)$, the diffusive particles in the vicinity of L have already reached L . So, the particles that contribute to the flux at L at this time are the ones that start from the center of the trap $x_0 = 0$ and reach L ballistically. The weight of such trajectories $\sim e^{-L^2/4Dt} \sim e^{-b^2/2\tau}$ makes the minimum around $\tau = \tau_1^* \sim O(1)$. In this regime where $1 \ll \tau \ll b^2$, the second term in (5) dominates.
- When $\tau \geq \tau_2^*$: For $t \sim L^2/2D$, i.e., $\tau \sim \tau_2^* \sim O(b^2)$, the particles that hit L for the first time are the typical trajectories that start from the most populated initial region near $x_0 = 0$ and arrive via diffusion to L . Finally when $\tau \gg \tau_2^*$, the first-passage flux to L are caused by trajectories that start from the trap center but take much

longer times to reach L due to their sojourns in the direction opposite to L .

When $b \rightarrow b_c$ from above, the two time scales τ_1^* and τ_2^* merge, the atypical ballistic trajectories disappear and the averaged FPTD is controlled entirely by diffusion — causing thus a dynamical phase transition at $b = b_c$ where the two time scales merge.

How robust is this dynamical phase transition? Does it occur for generic initial conditions, or is it something special for the Gaussian case? In fact, consider a generic initial condition with a finite width σ such that, $\mathcal{P}(x_0) = (1/\sigma)g(x_0/\sigma)$, where $g(y)$ is assumed to have an unbounded support on $y \in [-\infty, \infty]$. Then the integral in (3) can still be expressed in the scaling form in (4), with the scaling function given by

$$\Phi(\tau, b) = \frac{\sqrt{2}}{\sqrt{\pi\tau}} \int_{-\infty}^{\infty} dz |z| e^{-z^2} g(b - \sqrt{2\tau}z). \quad (6)$$

In the limit $\tau \rightarrow 0$, we get

$$\Phi(\tau, b) \approx \frac{\sqrt{2}g(b)}{\sqrt{\pi\tau}} \quad \text{as } \tau \rightarrow 0. \quad (7)$$

Thus, for generic unbounded initial condition, the scaling function diverges *universally* as $\tau^{-1/2}$ as $\tau \rightarrow 0$. Furthermore, it is not difficult to see that for any such initial condition $g(y)$, the dynamical transition at some critical b_c will also exist. As an example, we consider $g(y) = e^{-|y|}/2$ (double-exponential initial condition), for which the scaling function can be computed explicitly

$$\Phi(\tau, b) = \frac{e^{-b}}{4} \left[\sqrt{\frac{8}{\pi\tau}} + 2e^{\tau/2} \operatorname{erf}\left(\sqrt{\frac{\tau}{2}}\right) - e^{\tau/2} \left(\operatorname{erfc}\left(\frac{b-\tau}{\sqrt{2\tau}}\right) + e^{2b} \operatorname{erfc}\left(\frac{b+\tau}{\sqrt{2\tau}}\right) \right) \right]. \quad (8)$$

When plotted again τ (not shown here), the scaling function again exhibits a horizontal S-shaped form as in Fig. (2) with a minimum at $\tau_1^* \sim O(1)$ and a maximum at $\tau_2^* \sim O(b^2)$ for $b > b_c \approx 2.526$. The two time scales merge at $b = b_c$ again causing a dynamical phase transition. Hence we conclude that this transition is robust and occurs for any generic unbounded initial condition.

Is this transition restricted only to one dimension? From the general physical picture of the problem, it is clear that this transition should exist even in higher dimensions. In $d > 1$, it is necessary to have a target of a finite ‘tolerance’ size R_{tol} , because Brownian trajectories will surely miss a point target for $d > 1$. Thus we have an additional time scale $t_3^* = R_{\text{tol}}^2/2D$. But for fixed R_{tol} , the dynamical transition at some σ_c should exist. While the averaged FPTD in $d > 1$ can in principle be computed analytically, the calculations are somewhat tedious. However, we have checked numerically that this transition exists for $d = 2$, by integrating the Langevin equations: $\dot{x}(t) = \sqrt{2D}\eta_x(t)$ and $\dot{y}(t) = \sqrt{2D}\eta_y(t)$, where η_m ($m = x, y$) are white noises with $\langle \eta_m(t)\eta_{m'}(t') \rangle = \delta(t-t')\delta_{mm'}$. The simulation starts with $\{x(0), y(0)\}$ randomly extracted from a 2d

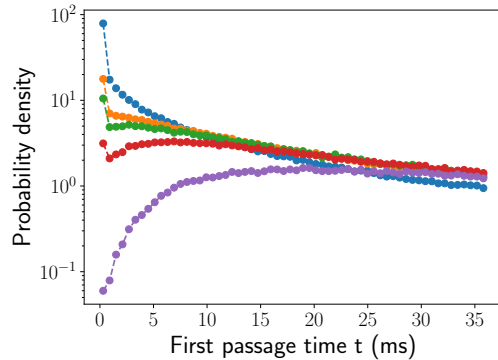


FIG. 3: 2d numerical simulation of the average FPTD for $b = 8, 5.5, 4.5, 4$ and 2 (from bottom to top) illustrating the dynamical transition in 2d around $b_c \approx 4.5$ for $a = 0.5$. Plotted for the experimental values $D = 1.5 \times 10^{-13} \text{ m}^2 \cdot \text{s}^{-1}$ and $\sigma = 36 \text{ nm}$.

Gaussian distribution of standard deviation σ and the first passage time is computed when the particle arrives within R_{tol} of the target. We fixed $a = R_{\text{tol}}/L = 0.5$ and simulated 5×10^6 trajectories with an integration step of $\approx 50 \mu\text{s}$. The average FPTD $\bar{F}_{2d}(t, b, a = 0.5)$ is computed from $\approx 10^6$ first passage times and plotted in Fig. 3. As in the 1d case the average FPTD changes with b from a monotonically decreasing function at $b < b_c$ to a distribution with a minimum and a maximum for $b > b_c$ with $b_c \approx 4.5$ here.

Finally, how general is this two-peaked structure of FPTD and its associated dynamical phase transition? Here we presented a simple scenario of free diffusion starting from an initial condition with a finite width σ , and we have shown the robustness of this transition with respect to different initial conditions as well as the spatial dimension d . Does the dynamical transition in FPTD persist for processes beyond simple diffusion? For example, consider a particle moving in an external confining potential in 1d, such as in the Ornstein-Uhlenbeck (OU) process where $dx/dt = -\mu x + \sqrt{2D}\eta(t)$: can one still see this transition in FPTD? The answer is indeed yes. An external confining potential induces, in addition to the two time scales $t_1^* \sim O(\sigma^2/D)$ and $t_2^* \sim O(L^2/D)$, a third time scale τ_{relax} corresponding to the relaxation time, e.g., in the OU process $\tau_{\text{relax}} = 1/\mu$. As long as $\tau_{\text{relax}} \gg \max(t_1^*, t_2^*)$, one would still see the competition between t_1^* and t_2^* and the dynamical transition when they merge. The algebraic tail of the FPTD for large t corresponding to free diffusion just gets cut-off by an exponential tail for $t \gg \tau_{\text{relax}}$. However, it doesn't affect the short time dynamical phase transition coming from the interplay between t_1^* and t_2^* . We have confirmed this general picture with experimental data and simulations (see the Supp. Mat. [36]). Of course, if the confining potential is very steep $\mu \gg 1$, i.e., when τ_{relax} becomes comparable to t_1^* or t_2^* , new behaviors of FPTD may emerge depending on the details of the trap. However, the two-peak behavior of FPTD and its associated dynamical transition is robust as long as the confining potential is not too steep.

This work has been partially supported by the FQXi Foundation, Grant No. FQXi-IAF19-05, “Information as a fuel in colloids and superconducting quantum circuits.”

* E-mail me at: sergio.ciliberto@ens-lyon.fr

† E-mail me at: satya.majumdar@universite-paris-saclay.fr

- [1] S. Redner, *A Guide to First-Passage Processes* (Cambridge University Press, 2001).
- [2] *First-Passage Phenomena and Their Applications*, Eds. R. Metzler, G. Oshanin, S. Redner (World Scientific, Singapore, 2013).
- [3] P. Hänggi, P. Talkner, and M. Borkovec, *Reaction-rate theory: fifty years after Kramers*, Rev. Mod. Phys. **62**, 251 (1990).
- [4] S. Reuveni, M. Urbakh, and J. Klafter, *Role of substrate unbinding in Michaelis–Menten enzymatic reactions*, Proc. Natl. Acad. Sci. USA **111**, 4391 (2014).
- [5] S. N. Majumdar, *Persistence in nonequilibrium systems*, Curr. Sci. **77**, 370 (1999).
- [6] A. J. Bray, S. N. Majumdar, and G. Schehr, *Persistence and first-passage properties in nonequilibrium systems*, Adv. in Phys. **62**, 225 (2013).
- [7] O. Bénichou, C. Loverdo, M. Moreau, and R. Voituriez, *Intermittent search strategies*, Rev. Mod. Phys. **83**, 81 (2011).
- [8] M. R. Evans, S. N. Majumdar, and G. Schehr, *Stochastic resetting and applications*, J. Phys. A: Math. Theor. **53**, 193001 (2020).
- [9] S. N. Majumdar, A. Pal, and G. Schehr, *Extreme value statistics of correlated random variables: A pedagogical review*, Phys. Rep. **840**, 1 (2020).
- [10] S. N. Majumdar and R.M. Ziff, *Universal Record Statistics of Random Walks and Lévy Flights*, Phys. Rev. Lett., **101**, 050601 (2008).
- [11] S. N. Majumdar, *Universal first-passage properties of discrete-time random walks and Lévy flights on a line: Statistics of the global maximum and records*, Physica A, **389**, 4299 (2010).
- [12] C. Godrèche, S. N. Majumdar and G. Schehr, *Record statistics of a strongly correlated time-series: Random Walks and Lévy Flights*, J. Phys. A: Math. Theor. **50**, 333001 (2017) .
- [13] A. Godec and R. Metzler, *First passage time distribution in heterogeneity controlled kinetics: going beyond the mean first passage time*, Sci. Rep. **6**, 20349 (2016).
- [14] J. Shin and A. B. Kolomeisky, *Target search on DNA by interacting molecules: First-passage approach*, J. Chem. Phys. **151**, 125101 (2019).
- [15] D. S. Grebenkov, D. Holcman, and R. Metzler, *Preface: new trends in first-passage methods and applications in the life sciences and engineering*, J. Phys. A: Math. Theor. **53**, 190301 (2020).
- [16] S. Chandrasekhar, *Stochastic problems in physics and astronomy*, Rev. Mod. Phys. **15**, 1 (1943).
- [17] S. N. Majumdar, *Brownian Functionals in Physics and Computer Science*, Curr. Sci. **89**, 2076 (2005).
- [18] M. R. Evans and S. N. Majumdar, *Diffusion with stochastic resetting*, Phys. Rev. Lett. **106**, 160601 (2011).
- [19] M. R. Evans and S. N. Majumdar, *Diffusion with optimal resetting*, J. Phys. A: Math. Theor. **44**, 435001 (2011).
- [20] M. R. Evans and S. N. Majumdar, *Diffusion with resetting in arbitrary spatial dimension*, J. Phys. A: Math. Theor. **47**, 285001 (2014).
- [21] L. Kuśmiercz, S. N. Majumdar, S. Sabhapandit, and G. Schehr, *First order transition for the optimal search time of Lévy flights with resetting*, Phys. Rev. Lett. **113**, 220602 (2014).
- [22] S.N. Majumdar, S. Sabhapandit, and G. Schehr, *Dynamical transition in the temporal relaxation of stochastic processes under resetting*, Phys. Rev. E, **91**, 052131 (2015).
- [23] A. Nagar and S. Gupta S, *Diffusion with stochastic resetting at power-law times*, Phys. Rev. E **93**, 060102 (R) (2016).
- [24] A. Pal, A. Kundu, and M. R. Evans, *Diffusion under time-dependent resetting*, J. Phys. A: Math. Theor. **49**, 225001 (2016).
- [25] U. Bhat, C. De Bacco, and S. Redner, *Stochastic search with Poisson and deterministic resetting*, J. Stat. Mech. **083401** (2016).
- [26] O. Tal-Friedman, A. Pal, A. Sekhon, S. Reuveni, and Y. Roichman, *Experimental realization of diffusion with stochastic resetting*, J. Phys. Chem. Lett. **11**, 7350 (2020).
- [27] B. Besga, A. Bovon, A. Petrosyan, S. N. Majumdar, and S. Ciliberto, *Optimal mean first-passage time for a Brownian searcher subjected to resetting: experimental and theoretical results*, Phys. Rev. Res. **2**, 032029 (2020).
- [28] S. Reuveni, *Optimal stochastic restart renders fluctuations in first passage times universal*, Phys. Rev. Lett. **116**, 170601 (2016).
- [29] M. R. Evans and S. N. Majumdar, *Effects of refractory period on stochastic resetting*, J. Phys. A: Math. Theor. **51** 475003 (2018).
- [30] A. Masó-Puigdellosas, D. Campos, and V. Méndez, *Transport properties and first-arrival statistics of random motion with stochastic reset times*, Phys. Rev. E **99**, 012141 (2019).
- [31] A. S. Bodrova and I. M. Sokolov, *Resetting processes with non-instantaneous return*, Phys. Rev. E **101**, 052130 (2020).
- [32] G. Mercado-Vásquez, D. Boyer, S. N. Majumdar, and G. Schehr, *Intermittent resetting potentials*, J. Stat. Mech. **113203** (2020).
- [33] D. Gupta, C. A. Plata, A. Kundu, and A. Pal, *Stochastic resetting with stochastic returns using external trap*, J. Phys. A: Math. Theo. **54**, 025003 (2021).
- [34] I. A. Martínez, A. Petrosyan, D. Guéry-Odelin, E. Trizac, and S. Ciliberto, *Engineered swift equilibration of a Brownian particle*, Nat. Phys. **12**, 843 (2016).
- [35] M. Chupeau, B. Besga, D. Guéry-Odelin, E. Trizac, A. Petrosyan, and S. Ciliberto *Thermal bath engineering for swift equilibration*, Phys. Rev. E **98**, 010104(R) (2018)
- [36] Supplemental Material presents the FPT probability distributions of the OU processes in a harmonic potential, computed using experimental and numerical data.

Supplementary Material of the Letter: Dynamical phase transition in the first-passage probability of a Brownian motion

B. Besga, F. Faisant, A. Petrosyan, S. Ciliberto*
*Univ Lyon, ENS de Lyon, Univ Claude Bernard, CNRS,
 Laboratoire de Physique, UMR 5672, F-69342 Lyon, France*

Satya N. Majumdar
LPTMS, CNRS, Univ. Paris-Sud, Université Paris-Saclay, UMR 8626, 91405 Orsay, France
 (Dated: April 20, 2021)

We report the numerical and experimental results for the probability distribution of the first-passage times (FPTD) for a particle confined in a harmonic potential discussed in the main text of the Letter.

At the end of the main text we discuss the properties of the FPTD when the particle is confined by a potential. The main claim is that in the case of confinement there are three characteristic times. Indeed, in addition to the two time scales $t_1^* \sim O(\sigma^2/D)$ and $t_2^* \sim O(L^2/D)$, there is a third time scale τ_{relax} corresponding to the relaxation time inside the potential well. As long as $\tau_{\text{relax}} \gg \max(t_1^*, t_2^*)$, one would still see the competition between t_1^* and t_2^* and the dynamical transition of the FPTD when they merge.

In order to check this claim we study numerically the Brownian motion of a colloid confined in a harmonic potential. Namely we integrate the Langevin equation :

$$\frac{dx}{dt} = -\frac{x}{\tau_{\text{relax}}} + \sqrt{2D} \eta(t) \quad (1)$$

where η is a delta correlated Gaussian noise with zero mean. The variance of x is $\sigma_x^2 = D\tau_{\text{relax}}$ in the stationary state. We fix $D = 1$ and $t_1 = 1$ which implies that the initial distribution of x_0 around $x = 0$ is kept constant with standard deviation $\sigma = 1$. We study the FPTD at $\tau_{\text{relax}}/t_1 = 17.6$ (corresponding to experimental parameters see below) and different values of $t_2 \sim L^2/D$ which is changed by varying the distance to the target L , i.e $b = L/\sigma$. The results are compared with those of the free particle in Fig.1. This figure shows that when τ_{relax} is larger than t_1 and t_2 the FPTD is not changed with respect to that of a free particle and the transition occurs at $b \simeq b_c$.

We confirm this observation using the experimental data of a weakly confined Brownian particle for which the trapping laser power was not zero (free diffusion) but was kept very small, getting $\tau_{\text{relax}} = 0.15$ s. As in the

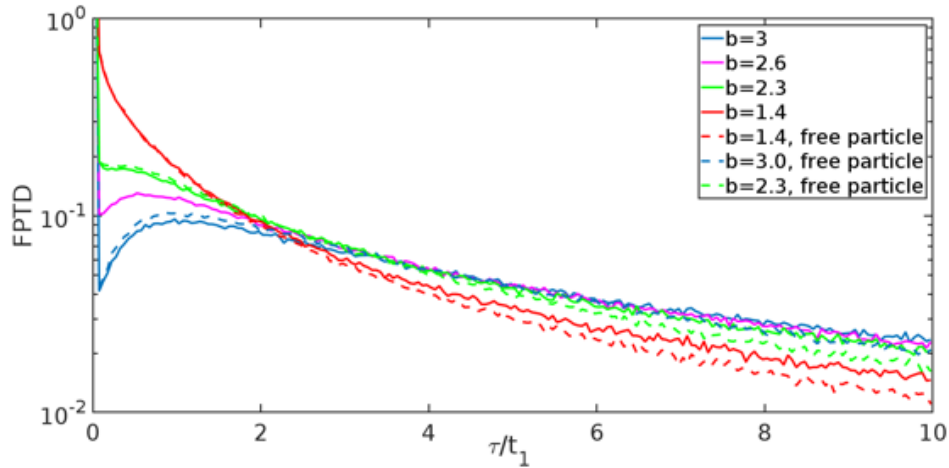


FIG. 1: FPTD (continuous lines) of the OU dynamics defined by Eq. (1) are compared with free diffusing particle (dashed lines) at $t_1 = 1$, $\tau_{\text{relax}}/t_1 = 17.6$ and at the same b of used in fig.2 of the main text.

*E-mail me at: sergio.ciliberto@ens-lyon.fr

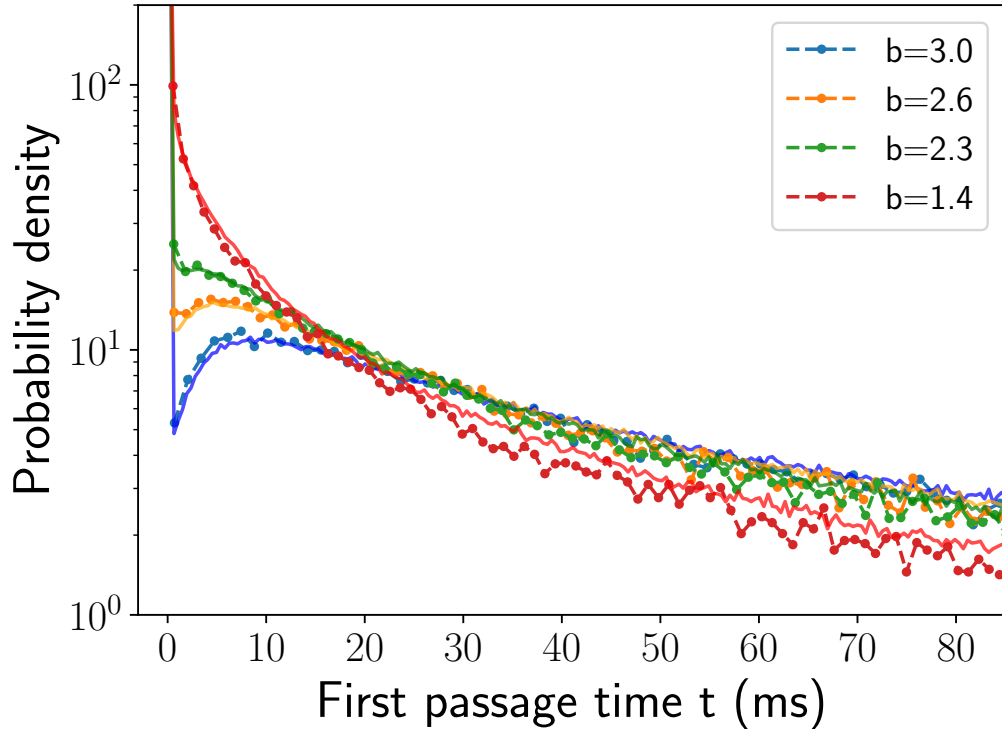


FIG. 2: The experimental data of the FPTD in the case of the OU dynamics are compared with the result of the numerical integration of Eq. (1) at $\tau_{\text{relax}}/t_1 = 17.6$ and various b indicated in the legend.

experiment $t_1 = 8.6$ ms we find that $\tau_{\text{relax}}/t_1 = 17.6$ as for the numerical results of Fig.1. In Fig.2 we compare the results of the numerical simulation of Eq.1 with the experimental values. The agreement is rather good.

These simple examples of FPTD in the motion of a particle confined in a harmonic potential prove that the transition in the FPTD is not a prerogative of free diffusion but it is a general property of the FPTD.

However τ_{relax} affects the FPTD when it becomes of the order of t_2 . We study the FPTD for two values of the ratio τ_{relax}/t_1 and two values of b . The results are compared with those of the free particle in Figs.3 a),b) for two values of b . These two figures confirm that as soon as τ_{relax} is larger than t_1 and t_2 the FPTD is very weakly affected with respect to that of a free particle. Instead the effect of the confinement is relevant when τ_{relax} is of the order of t_2 .

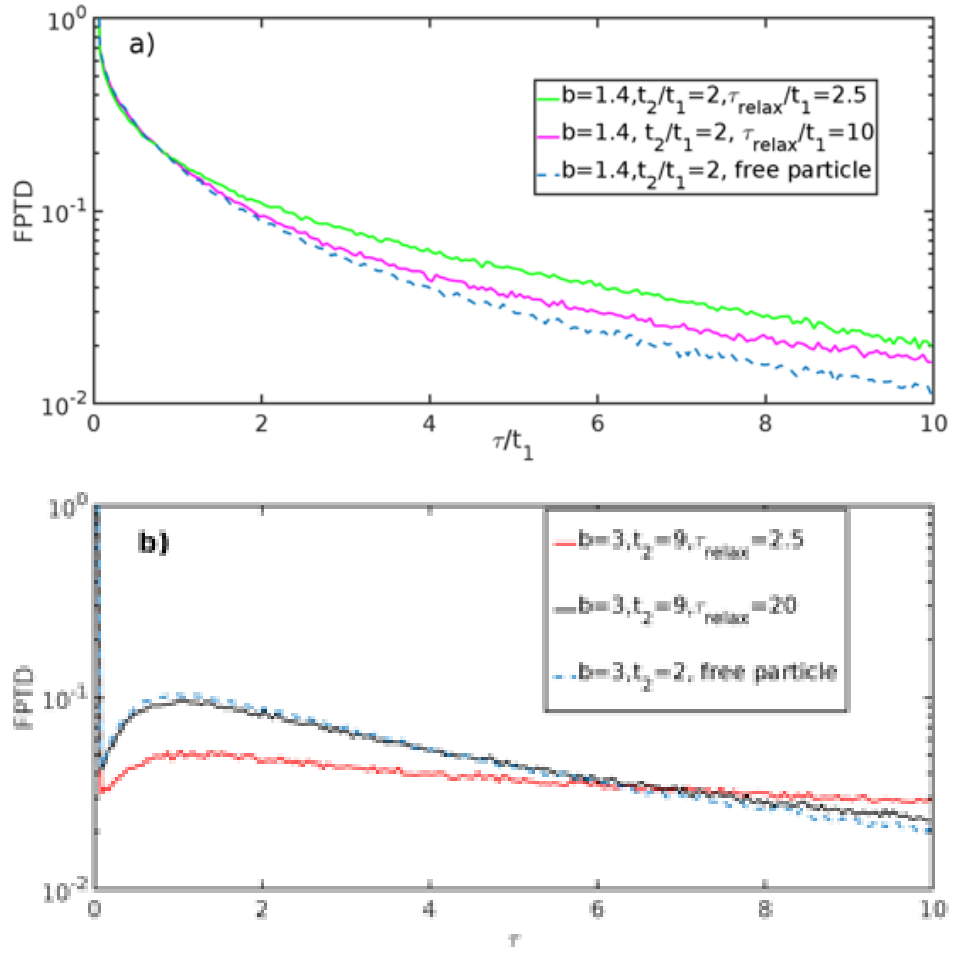


FIG. 3: FPTD of the OU dynamics defined by Eq. (1) are compared with a free diffusing particle at $t_1 = 1$ and various τ_{relax}/t_1 . The other parameters are $b = 1.4, t_2/t_1 = 2$ (a) and $b = 3, t_2/t_1 = 9$ (b)

